

## Pion absorption on polarized nuclear targets

Mohammad G. Khayat, N. S. Chant, and P. G. Roos

*Department of Physics, University of Maryland, College Park, Maryland 20742*

T.-S. H. Lee

*Argonne National Laboratory, Argonne, Illinois 60439*

(Received 21 July 1992)

The availability of polarized nuclear targets for nuclear reaction studies offers new research directions. In this paper we present the distorted wave impulse approximation formalism and calculations for two-nucleon pion absorption on polarized nuclear targets. We assume that the pion absorbs on a  ${}^3S_1$   $n$ - $p$  pair and use phenomenological amplitudes to describe the  $\pi NN$  vertex. The effects of the distortions on the incoming pion and outgoing protons, in contrast to the elementary  $\pi NN$  vertex, are delineated for certain special cases in which the formalism simplifies. Predictions of cross sections and vector and tensor analyzing powers are made for polarized target nuclei  ${}^6\text{Li}$ ,  ${}^7\text{Li}$ ,  ${}^{13}\text{C}$ , and  ${}^{14}\text{N}$  at pion incident energies of 115, 165, and 255 MeV.

PACS number(s): 25.80.Ls, 24.10.Eq, 24.70.+s

### I. INTRODUCTION

Recent advances in the technology of polarized targets have made available several new nuclear targets with sufficient polarization to permit studies of nuclear reactions. This development has led in turn to a series of experiments, or proposed experiments, in which spin observables are measured. Due to interference effects, spin observables are generally more sensitive to small terms in the transition amplitude than are unpolarized cross-section measurements. Thus one hopes to obtain a more complete understanding of either the reaction dynamics or the underlying nuclear structure or response function.

A particular area of interest is reactions with the spin zero pions. Initial measurements have concentrated on pion elastic scattering, for example,  ${}^3\text{He}$  [1],  ${}^6\text{Li}$  [2],  ${}^{13}\text{C}$  [3], and  ${}^{15}\text{N}$  [4], although some inelastic scattering data are available [2]. In addition, one measurement of the charge exchange reaction  ${}^{13}\text{C}(\pi^+, \pi^0){}^{13}\text{N}$  [5] has been made. Theoretical calculations of these processes have had limited success. These calculations show sensitivity to both the reaction model and the nuclear structure.

Other possible pion-induced nuclear reaction studies with polarized targets have not been studied experimentally, but theoretical studies have been made. Siegel and Gibbs [6] have carried out calculations for the  $(\pi^+, \eta)$  reaction and pointed out the importance of the so-called Newns [7] polarization which arises from the differential attenuation of the incoming and outgoing particles. Chant and Roos [8] have examined spin observables for the case of nucleon knockout by a pion from a polarized nuclear target. In these cases one obtains contributions to the vector analyzing power from both the two-body  $\pi$ -nucleon interaction and the differential attenuation of the incident and emitted particles.

In the present work we will consider pion absorption by a polarized nuclear target. We emphasize that the pion absorption mechanism is not well understood. In

particular, the previous distorted wave impulse approximation (DWIA) calculations [9–11] of the  $A(\pi^+, 2p)B$  reaction have been rather successful in predicting the dependence on kinematic variables. However, there is a major discrepancy in the magnitude of the cross section. The cause of this discrepancy is not understood, and may rise in part from nuclear structure limitations and in part from the reaction model. The separation of these effects is essentially impossible based on cross section data alone. The polarization observables will provide useful information for resolving the difficulties.

Our goal in this work is to provide guidance for the design of pion absorption measurements using polarized targets. We will carry out “baseline” calculations of cross sections and analyzing powers for several exclusive  $\vec{A}(\pi^+, 2p)B$  reactions. To do so, we adapt the DWIA formulation of Chant and Roos [9]. It is assumed that pion absorption occurs on a pair of nucleons in the target nucleus, and the incident pion and outgoing protons are strongly distorted by optical model potentials. We will elucidate the role of the contributions from these two different dynamical effects. Note that possible three-body absorption mechanisms, as suggested by recent measurements on  ${}^3\text{He}$  [12–14], do not directly induce nuclear transitions in the exclusive  $\vec{A}(\pi^+, 2p)B$  reaction. Within the DWIA, such effects are assumed to be included in the pion optical potential.

To predict the polarization observables within the two-nucleon absorption model it would be desirable to expand microscopic wave functions for the two participating target nucleons in terms of a complete set of states of relative motion, each to be associated with a corresponding two-particle absorption amplitude generated microscopically (details are given in Sec. II). This approach has been used by Ohta, Thies, and Lee [15]. However, the existing  $\pi NN$  models which have been reviewed by Garcilazo and Mizutani [16] have not been very successful in describing the polarization observables

in the  $\pi^+d \rightarrow pp$  reaction and are, therefore, unlikely to lead to satisfactory results in more complicated nuclear systems. We have noted previously that two-nucleon pion absorption is dominated by absorption on  ${}^3S_1$   $pn$  pairs. If we retain only this term, we can use the phenomenological amplitudes determined by Bugg, Hasan, and Shypit (BHS amplitudes) [17] which reproduce the observed  ${}^2\bar{H}(\pi^+, 2p)$  analyzing powers quite well, and hence should be much more satisfactory for predicting polarization observables for heavier targets. The use of these empirical amplitudes, instead of a single amplitude corresponding to the dominant  $s$ -wave  $\Delta$ - $N$  motion,

characterizes a major difference between the present calculations and our previous works on pion absorption. Clearly, this improvement is essential for the prediction of spin observables. In addition, the use of these amplitudes modifies somewhat the unpolarized cross section, as will be presented for the  ${}^{16}\text{O}(\pi^+, 2p){}^{14}\text{N}$  reaction.

In Sec. II we present the DWIA formalism and derive expressions for special cases of transitions in which the distortion effects can be most clearly examined. In Sec. III we present a series of calculations for the polarized nuclei  ${}^{14}\text{N}$ ,  ${}^6\text{Li}$ ,  ${}^7\text{Li}$ , and  ${}^{13}\text{C}$ . A summary of the results is given in Sec. IV.

## II. FORMALISM

Following Chant and Roos [9], we write the cross section for two-nucleon absorption on a nucleus with total angular momentum  $J_A$ , projection  $M_A$ , leading to a final nucleus with total angular momentum  $J_B$  as

$$\sigma_{BA}(M_A) = \frac{2\pi}{\hbar v} \omega_B c^2 \sum_{\substack{M_B \\ \rho'_c \rho''_d}} \left| \sum_{\substack{(n_1 l_1 j_1)(n_2 l_2 j_2) \\ \alpha \Lambda' m \sigma'_c \sigma''_d M}} \langle n_1 l_1 j_1 \rangle \langle n_2 l_2 j_2 \rangle \langle L' J L S J \rangle (-1)^{L'+l+J+S} \hat{L}' \hat{L} \hat{J} g_{AB}^{1/2} [(n_1 l_1 j_1)(n_2 l_2 j_2); JT] \right. \\ \times \left. \begin{array}{c} \left[ \begin{array}{ccc} l_1 & l_2 & L \\ \frac{1}{2} & \frac{1}{2} & S \\ j_1 & j_2 & J \end{array} \right] \left\{ \begin{array}{ccc} L' & l & L \\ S & J & j \end{array} \right\} (L' \Lambda' j m | J M) (J M J_B M_B | J_A M_A) T_{\sigma'_c \sigma''_d}^{\alpha L' \Lambda'} \\ \rho'_c \rho''_d \end{array} \right|^2 \\ \times \langle \mathbf{k}' ; \sigma'_c \sigma''_d ; \tau_c \tau_d | t^\alpha | \mathbf{k} ; l S j m ; T N \rangle \quad (1)$$

where  $\langle \mathbf{k}' ; \sigma'_c \sigma''_d ; \tau_c \tau_d | t^\alpha | \mathbf{k} ; l S j m ; T N \rangle$  is the amplitude for pion absorption on a  $pn$  pair in the state  $|\alpha l S j m \rangle$  leading to nucleons with spin projection  $\sigma'_c, \sigma''_d$ ,

$$T_{\sigma'_c \sigma''_d}^{\alpha L' \Lambda'} = \frac{1}{(2L'+1)^{1/2}} \int \chi_{\sigma'_c \rho'_c}^{(-)*} \chi_{\sigma''_d \rho''_d}^{(-)*} \chi^{(+)} G_{\Lambda'}^{\alpha L'} d^3 R, \quad (2)$$

and other quantities are defined in Ref. [9]. The details of the computation of  $G_{\Lambda'}^{\alpha L'}(\mathbf{R})$  are also outlined there. It is

significant that the sum over  $\alpha l S j m$  is coherent.

In the energy region near the  $\Delta$  resonance, it was found in Refs. [9] and [15] that the  $(\pi^+, 2p)$  reaction is dominated by the absorption on a deuteronlike  $l=0, S=j=1$  nucleon pair. In the calculations which follow we will retain only these quantum numbers in evaluating Eq. (1). This will permit us to calculate the absorption matrix element  $\langle |t^\alpha| \rangle$  using the BHS amplitudes for  $\pi^+d \rightarrow pp$ . Thus we obtain

$$\sigma_{BA}(M_A) = \frac{2\pi}{\hbar v} \omega_B c^2 \sum_{\substack{M_B \\ \rho'_c \rho''_d}} \left| \sum_{\substack{(n_1 l_1 j_1)(n_2 l_2 j_2) \\ \Lambda \Sigma \sigma'_c \sigma''_d M}} \langle n_1 l_1 j_1 \rangle \langle n_2 l_2 j_2 \rangle \langle L S J \rangle g_{AB}^{1/2} [(n_1 l_1 j_1)(n_2 l_2 j_2); JT] \right. \\ \times \left. \begin{array}{c} \left[ \begin{array}{ccc} l_1 & l_2 & L \\ \frac{1}{2} & \frac{1}{2} & S \\ j_1 & j_2 & J \end{array} \right] \hat{L} (L \Lambda \Sigma | J M) \\ (J M J_B M_B | J_A M_A) T_{\sigma'_c \sigma''_d}^{\alpha L \Lambda} \langle \mathbf{k}' ; \sigma'_c \sigma''_d ; \tau_c \tau_d | t^\alpha | \mathbf{k} ; S \Sigma ; T N \rangle \\ \rho'_c \rho''_d \end{array} \right|^2 \quad (3)$$

and

$$T_{\sigma'_c \sigma''_d}^{\alpha L \Lambda} = \frac{1}{(2L+1)^{1/2}} \int \chi_{\sigma'_c \rho'_c}^{(-)*} \chi_{\sigma''_d \rho''_d}^{(-)*} \chi^{(+)} G_{\Lambda}^{\alpha L} d^3 R, \quad (4)$$

where the two-nucleon quantum numbers  $l S j m$  are sim-

ply replaced by the spin angular momentum  $S \Sigma$  and  $S=1$ . These are the expressions which are coded in the calculations which follow.

For a given choice of absorption matrix element  $\langle |t| \rangle$  and nuclear spectroscopic factor  $S_{AB}$ , one can see from Eqs. (3) and (4) that the absorption cross sections depend

visibly on the distortion of the incoming pion and outgoing protons. It is, therefore, useful to consider special cases so that the distortion effects can be most clearly examined. These special cases can be obtained by assuming

(i) that spin-orbit distortions for the emitted protons may be ignored, and (ii) that only single values of  $L$  and  $J$  contribute to the transition. With these restrictions we can write

$$\sigma_{BA}(M_A) = \frac{2\pi}{\hbar v} \omega_B \sum_{M_B} \left| \sum_{\Lambda\Sigma M} (L\Lambda\Sigma|JM)(JM J_B M_B | J_A M_A) T_{BA}^{\alpha L \Lambda}(\mathbf{k}'; \rho'_c \rho''_d; \tau_c \tau_d | t^\alpha | \mathbf{k}; S\Sigma; TN) \right|^2, \quad (5)$$

where

$$T_{BA}^{\alpha L \Lambda} = \frac{1}{(2L+1)^{1/2}} \int \chi_c^{(-)*} \chi_d^{(-)*} \chi^{(+)} U(R) Y_{L\Lambda}(\hat{R}) d^3R \quad (6)$$

and, for convenience, we have absorbed any structure factors into  $U(R)$ , that is,

$$U(R) Y_{L\Lambda}(\hat{R}) = c \sum^{(n_1 l_1 j_1)(n_2 l_2 j_2)} g S_{AB}^{1/2}[(n_1 l_1 j_1)(n_2 l_2 j_2); JT] \begin{bmatrix} l_1 & l_2 & L \\ \frac{1}{2} & \frac{1}{2} & S \\ j_1 & j_2 & J \end{bmatrix} \sqrt{2L+1} G_\Lambda^{\alpha 0 L}(\mathbf{R}). \quad (7)$$

Expanding the sum over quantum numbers in Eq. (5), and omitting reference to isospin quantum numbers, we obtain

$$\begin{aligned} \sigma_{BA}(M_A) &= \frac{2\pi}{\hbar v} \omega_B \sum_{M_B \rho'_c \rho''_d} \sum_{\substack{\Lambda\Sigma, M \\ \Lambda'\Sigma'}} (JM J_B M_B | J_A M_A)^2 (L\Lambda\Sigma|JM)(L\Lambda'\Sigma'|JM) T_{BA}^{\alpha L \Lambda} T_{BA}^{\alpha L \Lambda'} \\ &\quad \times \langle \mathbf{k}'; \rho'_c \rho''_d | t^\alpha | \mathbf{k}; S\Sigma \rangle \langle \mathbf{k}'; \rho'_c \rho''_d | t^\alpha | \mathbf{k}; S\Sigma' \rangle^* \\ &= \sigma_{BA}^{\text{diag}}(M_A) + \sigma_{BA}^{\text{cross}}(M_A), \end{aligned} \quad (8)$$

where the two terms correspond to the diagonal and cross terms in the summation, which are

$$\sigma_{BA}^{\text{diag}}(M_A) = \frac{2\pi}{\hbar v} \omega_B \sum_{M_B \rho'_c \rho''_d} \sum_{\Lambda\Sigma M} (JM J_B M_B | J_A M_A)^2 (L\Lambda\Sigma|JM)^2 |T_{BA}^{\alpha L \Lambda}|^2 \langle \mathbf{k}'; \rho'_c \rho''_d | t^\alpha | \mathbf{k}; S\Sigma \rangle^2 \quad (9)$$

and

$$\begin{aligned} \sigma_{BA}^{\text{cross}}(M_A) &= \frac{2\pi}{\hbar v} \omega_B \sum_{M_B \rho'_c \rho''_d} \sum_{\substack{\Lambda \neq \Lambda', M \\ \Sigma \neq \Sigma'}} (JM J_B M_B | J_A M_A)^2 (L\Lambda\Sigma|JM)(L\Lambda'\Sigma'|JM) T_{BA}^{\alpha L \Lambda} T_{BA}^{\alpha L \Lambda'} \\ &\quad \times \langle \mathbf{k}'; \rho'_c \rho''_d | t^\alpha | \mathbf{k}; S\Sigma \rangle \langle \mathbf{k}'; \rho'_c \rho''_d | t^\alpha | \mathbf{k}; S\Sigma' \rangle^*. \end{aligned} \quad (10)$$

To display most clearly the physics content of our studies, we consider only coplanar reaction geometries with a target polarized normal to the scattering plane, chosen to be the axis of quantization ( $\hat{z}$ ). Furthermore, before considering calculations for specific nuclear transitions, we examine two cases in which Eq. (8) is particularly simplified. In these cases, of  $L=0$ ,  $J=1$  and  $L=1$ ,  $J=1$ , the roles of the  $\pi NN$  vertex and the distortion effects can be more clearly seen.

For  $L=0$  transitions the cross terms in Eq. (10) vanish. By summing over  $\rho'_c$  and  $\rho''_d$  and remembering that  $S=1$ , the cross section becomes

$$\begin{aligned} \sigma_{BA}^{L=0}(M_A) &= \frac{2\pi}{\hbar v} \omega_B \sum_{M_B \Sigma M} (JM J_B M_B | J_A M_A)^2 |T_{BA}^{00}|^2 \\ &\quad \times \sigma_{\pi d}(\Sigma), \end{aligned} \quad (11)$$

where  $\sigma_{\pi d}(\Sigma)$  is the free  $\pi^+ d \rightarrow pp$  cross section for a given deuteron spin projection  $\Sigma$ . We now note that the distortion effects are isolated in  $|T_{BA}^{00}|^2$ , which is independent of the magnetic quantum numbers  $M_B$ ,  $\Sigma$ , and  $M$  and hence can be taken outside of the summation. Thus,

$$\begin{aligned} \sigma_{BA}^{L=0}(M_A) &= \frac{2\pi}{\hbar v} \omega_B |T_{BA}^{00}|^2 \\ &\quad \times \sum_{M_B, \Sigma = M_A - M_B} (1 \Sigma J_B M_B | J_A M_A)^2 \sigma_{\pi d}(\Sigma). \end{aligned} \quad (12)$$

Using the above formula we can calculate polarization observables for specific initial and final nuclear spins. We use the following expressions for vector and tensor analyzing powers:

$$\begin{aligned}
A_y &= \frac{\sigma(+\frac{1}{2}) - \sigma(-\frac{1}{2})}{\sigma_{\text{tot}}}, \quad (J_A = \frac{1}{2}, 1), \\
A_{yy} &= [\sigma(+1) - \sigma(0) + \sigma(-1) - \sigma(0)] / \sigma_{\text{tot}} \quad (J_A = 1), \\
A_y &= \{[\sigma(\frac{3}{2}) - \sigma(-\frac{3}{2})] + \frac{1}{3}[\sigma(\frac{1}{2}) - \sigma(-\frac{1}{2})]\} / \sigma_{\text{tot}} \\
&\quad (J_A = \frac{3}{2}), \quad (13) \\
A_{yy} &= \{[\sigma(\frac{3}{2}) + \sigma(-\frac{3}{2})] - [\sigma(\frac{1}{2}) + \sigma(-\frac{1}{2})]\} / \sigma_{\text{tot}} \\
&\quad (J_A = \frac{3}{2}), \\
A_{yyy} &= \{\frac{1}{3}[\sigma(\frac{3}{2}) - \sigma(-\frac{3}{2})] - [\sigma(\frac{1}{2}) - \sigma(-\frac{1}{2})]\} / \sigma_{\text{tot}} \\
&\quad (J_A = \frac{3}{2}),
\end{aligned}$$

where  $\sigma_{\text{tot}} = \sum_m \sigma(m)$ .

Table I presents the results for specific transitions with  $L=0$ .

We note that for  $L=0$  the vector ( $A_y$ ) and tensor ( $A_{yy}$ ) target analyzing powers are simply related to the two-body  $\pi^+d \rightarrow pp$  analyzing powers and are independent of distortion effects. Thus, although the cross section will be strongly affected by distortion effects and the nuclear structure, the analyzing powers reflect the  $\pi$ - $NN$  vertex. Moreover, we will show in Sec. III that the inclusion of spin-orbit terms for the emitted proton wave

does not change this result significantly. We also note that there can be no rank 3 analyzing power, even for a spin  $\frac{3}{2}$  target.

As a second case in which the cross section simplifies, we consider  $L=1$  transitions. In the general case of  $L \neq 0$ , the cross sections can no longer be separated into a simple product of a distortion term (dynamics) and the two-body  $\pi^+d \rightarrow 2p$  cross sections. Coherent terms enter the expressions in Eqs. (8)–(10). However, the equations can be reduced somewhat in complexity by taking advantage of a symmetry property of the spherical harmonics, namely,

$$Y_{L\Lambda}(\theta, \phi) = (-1)^{L+\Lambda} Y_{L\Lambda}(\pi - \theta, \phi).$$

Using this property, and restricting our considerations to a coplanar geometry, the terms in  $T_{BA}^{\alpha L \Lambda}$  [see Eq. (6)] become mirror symmetric with respect to the scattering plane; therefore, for our choice of the axis of quantization, these terms are identical for  $\theta$  and  $\pi - \theta$ . This in turn leads to the following selection rule:  $T_{BA}^{\alpha L \Lambda} = 0$  if  $L + \Lambda$  is odd.

If we now consider a pure  $L=1$  transition starting with a spin-one ( $J_A=1$ ) target, use of the above selection rule leads to the following expressions for the differential cross sections for each substate of the target spin:

TABLE I. Cross sections and vector and tensor analyzing powers for  $L=0$  absorption only. For each case  $\kappa = (2\pi\omega_B / \hbar v) S_{BA} |T_{BA}^{00}|^2$ .

$J_A$	$J_B$	$\sigma_{BA} \left[ M_A = \begin{array}{c} +J_A \\ \vdots \\ -J_A \end{array} \right]$	$A_y^{BA}$	$A_{yy}^{BA}$	$A_{yyy}^{BA}$
1	0	$\kappa\sigma_{\pi d}(+1)$ $\kappa\sigma_{\pi d}(0)$ $\kappa\sigma_{\pi d}(-1)$	$A_y^{\pi d}$	$A_{yy}^{\pi d}$	
1	1	$\frac{1}{2}\kappa[\sigma_{\pi d}(+1) + \sigma_{\pi d}(0)]$ $\frac{1}{2}\kappa[\sigma_{\pi d}(+1) + \sigma_{\pi d}(-1)]$ $\frac{1}{2}\kappa[\sigma_{\pi d}(0) + \sigma_{\pi d}(-1)]$	$\frac{1}{2}A_y^{\pi d}$	$-\frac{1}{2}A_{yy}^{\pi d}$	
1	2	$(\kappa/10)[\sigma_{\pi d}(+1) + 3\sigma_{\pi d}(0) + 6\sigma_{\pi d}(-1)]$ $(\kappa/10)[\sigma_{\pi d}(+1) + 4\sigma_{\pi d}(0) + 3\sigma_{\pi d}(-1)]$ $(\kappa/10)[6\sigma_{\pi d}(+1) + 3\sigma_{\pi d}(0) + \sigma_{\pi d}(-1)]$	$-\frac{1}{2}A_y^{\pi d}$	$\frac{1}{10}A_{yy}^{\pi d}$	
$\frac{1}{2}$	$\frac{1}{2}$	$(\kappa/3)[2\sigma_{\pi d}(+1) + \sigma_{\pi d}(0)]$ $(\kappa/3)[\sigma_{\pi d}(0) + 2\sigma_{\pi d}(-1)]$	$A_y^{\pi d}$		
$\frac{1}{2}$	$\frac{3}{2}$	$\kappa[\frac{1}{6}\sigma_{\pi d}(+1) + \frac{1}{3}\sigma_{\pi d}(0) + \frac{1}{2}\sigma_{\pi d}(-1)]$ $\kappa[\frac{1}{2}\sigma_{\pi d}(+1) + \frac{1}{3}\sigma_{\pi d}(0) + \frac{1}{6}\sigma_{\pi d}(-1)]$	$-\frac{1}{2}A_y^{\pi d}$		
$\frac{3}{2}$	$\frac{1}{2}$	$\kappa\sigma_{\pi d}(+1)$ $(\kappa/3)[\sigma_{\pi d}(+1) + 2\sigma_{\pi d}(0)]$ $(\kappa/3)[2\sigma_{\pi d}(0) + \sigma_{\pi d}(-1)]$ $\kappa\sigma_{\pi d}(-1)$	$\frac{10}{12}A_y^{\pi d}$	$\frac{1}{2}A_{yy}^{\pi d}$	0

$$\begin{aligned}
\sigma_{BA}(M_A = \pm 1) &= \frac{1}{2} \kappa |T^{1\pm 1}|^2 \sigma_{\pi d}(0), \\
\sigma_{BA}(M_A = 0) &= \frac{1}{2} \kappa \left[ |T^{1-1}|^2 \sigma_{\pi d}(+1) + |T^{1+1}|^2 \sigma_{\pi d}(-1) \right. \\
&\quad \left. - T^{1-1} T^{11*} \sum_{\rho'_c \rho'_d} \langle \mathbf{k}' ; \rho'_c \rho'_d | t_f^\alpha | \mathbf{k}, 1, 1 \rangle \langle \mathbf{k}' ; \rho'_c \rho'_d | t_f^\alpha | \mathbf{k}, 1, -1 \rangle^* - \text{c.c.} \right], \tag{14}
\end{aligned}$$

where c.c. denotes the complex conjugate of the term preceding it, and  $\kappa = 2\pi\omega_B / \hbar v$ .

We immediately see that distortions have complicated the expressions considerably. However, we do obtain a relatively simple expression for  $A_y$ , namely,

$$\begin{aligned}
A_y &= \frac{1}{2} \kappa (|T^{11}|^2 - |T^{1-1}|^2) \frac{\sigma_{\pi d}(0)}{\sigma_{\text{tot}}^{BA}} \\
&= \frac{1}{2} \kappa (|T^{11}|^2 - |T^{1-1}|^2) \frac{\sigma_{\text{tot}}^{\pi d}}{3\sigma_{\text{tot}}^{BA}} (1 - A_{yy}^{\pi d}), \tag{15}
\end{aligned}$$

where  $\sigma_{\text{tot}} = \sum_M \sigma(M)$  as before.

This formula clearly suggests that if distortions are ignored then  $A_y = 0$  since  $|T^{11}|^2 = |T^{1-1}|^2$  in the plane-wave limit (PWIA). Thus, any observed vector analyzing power for  $L = 1$  is largely due to the effects of distortions in  $\bar{A}(\pi^+, 2p)B$  reactions. Similar effects arising from distortions are observed in  $(\pi, \pi p)$  [8] and  $(p, 2p)$  [18] reactions.

### III. DWIA CALCULATIONS

In performing these calculations we have modified the DWIA code THREDEE [8,9] to calculate the cross sections and analyzing powers of Eqs. (3) and (13). These calculations require a number of input parameters and data. Before considering specific calculations we specify the input.

The functions  $G_{\Lambda}^{\alpha 0L}$  describing the center-of-mass motion of the  ${}^3S_1$  pair in the nucleus, as contained in Eq. (4), were calculated microscopically as in Refs. [9–11]. The nuclear structure input was taken from published shell-model calculations or, in some cases, calculated from single configurations known to dominate the wave functions of the specific nuclear states. Using the resultant two-particle spectroscopic amplitudes for each transition, single-particle wave functions were generated using a Woods-Saxon potential with a geometry consistent with electron scattering [19] and with appropriate binding energies. These  $pn$  pair wave functions were then transformed to relative and center-of-mass coordinates and the overlap computed with the deuteron internal wave function. The resultant function describes the center-of-mass motion of that component of the target-residual nucleus overlap in which the relative motion of the  $pn$  pair is identical to the deuteron ground state.

The distorted waves for the outgoing protons were generated using the optical-model potentials determined in

the global studies by Nadasen *et al.* [20]. These potentials have been shown to produce reasonable results for protons in the 100–200 MeV energy range, even for light nuclei [21].

In the present work we restrict ourselves to pion energies  $115 \text{ MeV} < T_\pi < 260 \text{ MeV}$ ; the choice of the lower limit is primarily dictated by the fact that the observed polarization analyzing powers for  ${}^2\bar{H}(\pi^+, 2p)$  are very small for low energies; as discussed below, the upper limit is dictated by availability of detailed data for the two-body  $t$  matrix. For this energy range it is sufficient to calculate the incoming pion distorted wave using a Kisslinger-type pion optical-model potential with parameters from Cottingham and Holtkamp [22]. This potential has been used in our previous calculations and gives a rather good description of the kinematic dependences of the pion absorption data.

The  $\pi^+ d \rightarrow 2p$  amplitudes were taken from the work of Bugg and co-workers [17]. These BHS fitted amplitudes reproduce the experimental cross sections very well when compared to the compilation of Ritchie [23]. A spline interpolation was used to obtain the amplitudes for energies between those published. Because of the choice of data sets used in the fit, the available amplitudes are limited to pion energies below about 256 MeV.

In Sec. III A below we reinvestigate the  ${}^{16}\text{O}(\pi^+, 2p)$  reaction. We will examine the extent to which the previously published DWIA results [9–11] can be improved through the use of the BHS amplitudes. In Sec. III B we present detailed DWIA calculations for  ${}^{14}\bar{N}(\pi^+, 2p)$ , since  ${}^{14}\text{N}$  has been successfully polarized in the laboratory. The effects of distortions on the cross sections and polarization observables,  $A_y$  and  $A_{yy}$ , for the special cases discussed in Sec. II will be illustrated. Predictions for general cases with  $L > 0$  will also be presented, and the effects of the spin-orbit potential for the outgoing protons will be examined. In Sec. III C we calculate polarization observables for other targets which have been polarized or present an opportunity to investigate the effects of target spin on pion absorption reactions.

#### A. Results for ${}^{16}\text{O}(\pi^+, 2p){}^{14}\text{N}$

In the previous DWIA calculations of Refs. [9–11] the  $\pi NN$  matrix elements  $\langle |t| \rangle$  of Eq. (3) were calculated from a single amplitude corresponding to the formation of a  ${}^3S_2$   $\Delta$ - $N$   $s$ -wave state which then decays into a  ${}^1D_2$   $p$ - $p$  state. The nuclear transitions associated with other

possible  $pp$  partial waves were, therefore, neglected. This simplification is removed in the present work by using the empirical BHS amplitudes [17] to calculate the  $\pi NN$  matrix element. It is, therefore, interesting and important to investigate whether the use of the BHS amplitudes will remove the discrepancies between the previous DWIA predictions for the  $^{16}\text{O}(\pi^+, 2p)^{14}\text{N}$  reaction and the experimental data.

It is instructive to first illustrate the dynamical differences between the single amplitude and the BHS amplitudes by comparing the predictions of the  $J$  dependence of the cross sections. These results are presented in Fig. 1 for  $^{16}\text{O}(\pi^+, 2p)^{14}\text{N}$   $L=2$  transition to  $J^\pi=1^+$ ,  $2^+$ , and  $3^+$  states at 116 MeV. For each  $J$  we see that the use of BHS amplitudes changes significantly the calculated cross sections both in their magnitudes and shapes. More importantly, the  $J$  dependence calculated from BHS amplitudes is less pronounced. This implies that in calculations involving interference between amplitudes of different multiplicities, the predictions from using the BHS amplitudes can be very different from previous DWIA results.

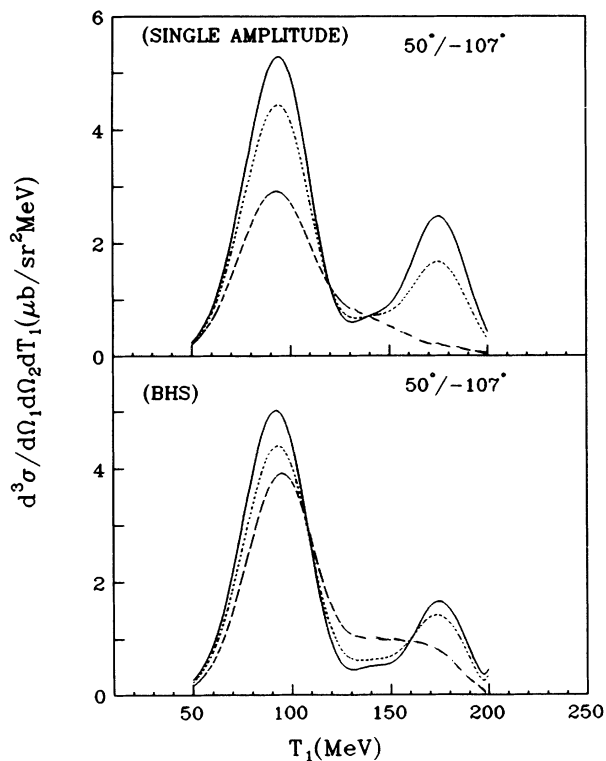


FIG. 1. DWIA  $L=2$  energy sharing distributions for  $^{16}\text{O}(\pi^+, 2p)^{14}\text{N}$  leading to  $1^+$  (full),  $2^+$  (dashed), and  $3^+$  (dotted) states using identical kinematics and structure. The proton angles of  $\theta_1=50^\circ$  and  $\theta_2=-107^\circ$  correspond to a quasifree setting. The top panel corresponds to the use of a single amplitude for the  $\pi^+ d \rightarrow pp$  vertex, and the lower panel to the use of the Bugg, Hasan, and Shypit [17] amplitudes. The top panel corresponds to the calculations shown in Fig. 3 of Ref. [9], but with a corrected two-body transform.

In Fig. 2 we compare the data of Schumacher *et al.* [11] with the DWIA calculations. The shell model of Cohen and Kurath [24] is used to calculate the needed nuclear structure amplitudes. The most notable improvement from using the BHS amplitudes is a better description of the shapes of the cross sections for the  $2^+(7.03 \text{ MeV})$  and  $3^+(11.0 \text{ MeV})$  states. However, the difficulty in describing the shape of the cross section for the transition to the  $1^+(0.0 \text{ MeV})$  state is not removed. This is not too surprising, since the Cohen-Kurath shell model wave functions are known to be inadequate for the  $1^+$  ground state of  $^{14}\text{N}$  from  $\beta$ -decay studies. This is because the limited model space considered does not account for important ground-state correlations involving more than  $1\hbar$  excitation.

In all cases, the calculated magnitudes of the cross sections are smaller than the data by a factor ranging from about 2 to 6. We note that the present DWIA calculations involve three distorted waves and, therefore, the predicted magnitudes of the cross sections are very sensitive to the accuracies of the employed optical potentials. The optical potentials used in this work are obtained from fitting only the elastic cross sections. As is well known, the distorted wave functions generated from such a phenomenological approach, which are used for calculating nuclear transitions matrix elements, could be inaccurate in the nuclear interior. It is one of the objectives of this paper to explore how the dynamics originating from optical potentials can be delineated by performing new experiments using polarized targets. The expressions for several special cases presented in Sec. II will be used in such discussions later.

On the theoretical side, the next step to improve the DWIA predictions would be to use optical potentials constructed from not only fitting elastic cross sections, but also taking into account important dynamical effects occurring inside the nucleus. For example, the  $\Delta$ -nucleus interaction, as described within the  $\Delta$ -hole model, should be included in the pion optical potential. Proton optical potentials constructed from the  $NN$   $G$  matrix may be essential for an accurate description of the outgoing proton distorted waves. Our efforts in this direction will be presented elsewhere. For present purposes of predicting polarization observables which depend on the ratio of cross sections, the DWIA model developed above should be sufficient.

## B. Predictions for the $^{14}\vec{\text{N}}(\pi^+, 2p)^{12}\text{C}$ reaction

Since the  $^{14}\text{N}$  nucleus has been successfully polarized in the laboratory, we will make predictions for guiding the design of an experiment on the  $^{14}\vec{\text{N}}(\pi^+, 2p)^{12}\text{C}$  reaction. The calculations have been carried out for kinematics such that one of the outgoing protons emerges at an angle of  $50^\circ$  with respect to the beam direction. This is chosen to maximize the analyzing power as suggested by the data of  $\pi^+ d \rightarrow pp$ . The second proton is taken to be at the corresponding quasifree angle for which zero recoil momentum of the residual nucleus is kinematically allowed. These angles are  $-107^\circ$ ,  $-105^\circ$ , and  $-99^\circ$  for the

considered incident pion energies of 115, 165, and 255 MeV, respectively.

Within the DWIA developed in Sec. II, the strength of a transition from the  $^{14}\text{N}(1^+)$  ground state to a state in  $^{12}\text{C}$  depends strongly on the orbital angular momentum  $L$  of the deuteronlike  $^3S_1$  pair in the  $^{14}\text{N}$  target nucleus. For the  $^{12}\text{C}$  ground state and first excited  $2^+(4.43\text{ MeV})$  state,  $L$  can be only 0 and 2. The only states which can be reached by an  $L=1$  transition are  $0^-2^-$  states at high excitation energy. Based on shell-model considerations, the excitation strengths for  $L > 2$  transitions are expected to be much weaker and are, therefore, not considered in this work.

It is useful to examine first the  $L$  dependence of the cross sections and analyzing powers. The  $L=0$  and 2 nuclear structure amplitudes for the  $^{12}\text{C}$  ground-state transition are taken from the shell model of Cohen and Kurath [24]. The  $L=1$  transition is assumed to be due to the removal of a  $1p_{1/2}1s_{1/2}$  pair of nucleons from  $^{14}\text{N}$ . As discussed in Sec. III A, we are particularly interested in the distortion effects and will, therefore, compare the DWIA and plane-wave impulse approximation (PWIA) results.

The results for  $L=0$  are displayed in Fig. 3. We observe that the distortion effects are considerable for the cross sections, reducing the magnitude by about a factor of 6 at the maximum and washing out the minima which arise in the PWIA calculation due to the nodes in the wave function. The analyzing powers are, however, unaffected by the distortion. This comes about because the  $L=0$  cross sections depend on a single nuclear matrix element  $|T_{BA}^{00}|^2$  as seen in Eq. (12). This nuclear reaction factor drops out in the calculation of the analyzing powers. Hence, the predictions of  $A_y$  and  $A_{yy}$  in Fig. 3 are simply related to the  $\pi^+d \rightarrow pp$  cross section  $\sigma_{\pi d}(\Sigma)$ .

Their variations with respect to the kinetic energy of the detected proton is due to the Fermi motion of the deuteronlike  $^3S_1$  pair.

In Fig. 4 we present calculations for the  $L=1$  transition. The PWIA cross sections (dashed curves) have the characteristic minimum at the kinematics corresponding to zero recoil momentum for the residual nucleus. These minima are almost totally filled in by the distortion effects. The overall effect of the distortion on the magnitude of the cross section is similar to that of the  $L=0$  cases. As seen in Eq. (15), the vector analyzing power is zero in the PWIA since  $|T^{11}|^2 = |T^{1-1}|^2$  in the absence of distortion effects. The predicted analyzing power is reasonably large. Its change in sign at the zero recoil momentum point corresponds to the fact that, at this point, the recoil nucleus direction reverses. The predicted  $A_{yy}$  is large and negative and the distortion effects are also significant.

The results for an  $L=2$  transition to the  $^{12}\text{C}$  ground state are shown in Fig. 5. The PWIA cross sections are similar to those in Fig. 4, with the minima at zero recoil momentum being more pronounced due to the fact that the two maxima are better separated in energy for higher  $L$  values. In this  $L=2$  case the expressions for the analyzing power no longer simplify, and we expect contributions from both distortion effects and the two-body  $\pi^+d \rightarrow pp$  analyzing power. Nevertheless, distortion plays the dominant role in generating a very large vector analyzing power  $A_y$ , as can be seen by comparing the DWIA (solid) and PWIA (dashed) results in Fig. 5. The effect of distortion on  $A_{yy}$  is much weaker, except near the minima.

We now turn to the presentation of predictions of realistic calculations using the coherent admixture of  $L=0$  and 2 specified by the model of Cohen and Kurath

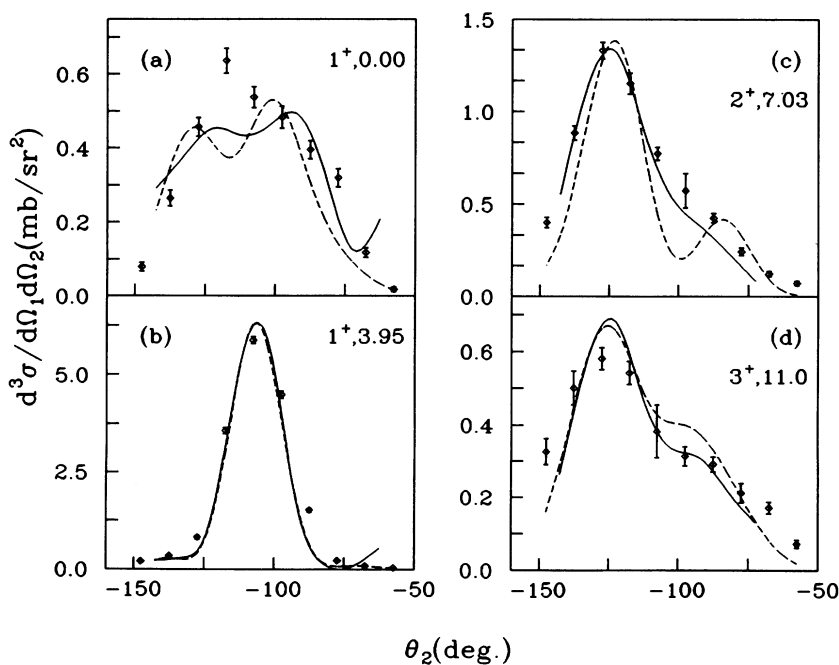


FIG. 2. Angular correlations for  $^{16}\text{O}(\pi^+, 2p)^{14}\text{N}$  with one proton fixed at  $50^\circ$  and for various final states [11]. The DWIA calculations correspond to the use of a single amplitude for  $\pi^+d \rightarrow pp$  (dashed lines) and the Bugg, Hasan, and Shypit [17] amplitudes (solid lines). The normalizations of the calculations are  $1^+$ , 0.00 MeV ( $S$ , 3.0;  $B$ , 3.4);  $1^+$ , 3.95 MeV ( $S$ , 6.7;  $B$ , 6.4);  $2^+$ , 7.03 MeV ( $S$ , 3.7;  $B$ , 4.2);  $3^+$ , 11.0 MeV ( $S$ , 1.9;  $B$ , 1.7), where  $S$  and  $B$  refer to single amplitude and Bugg, Hasan, and Shypit amplitudes, respectively.

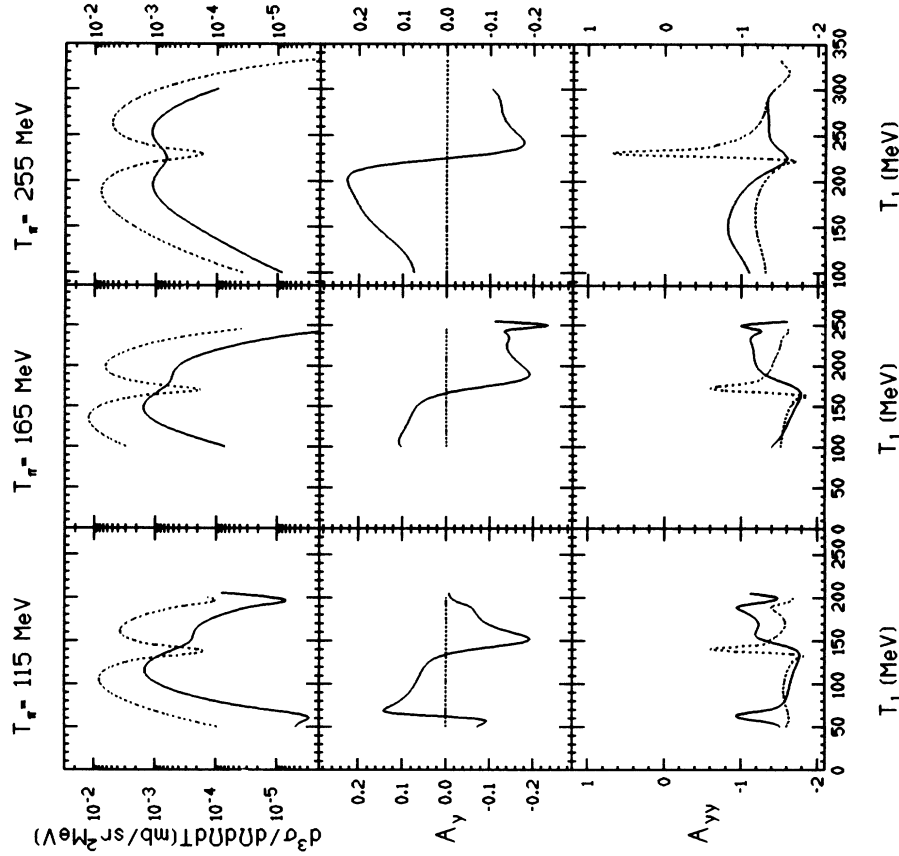


FIG. 3. Energy sharing cross sections, vector analyzing powers ( $A_y$ ), and tensor analyzing powers ( $A_{yy}$ ) for  $^{14}\text{N}(\pi^+, 2p)^{12}\text{C}(0^+)$  with  $L=0$  transfer. The curves correspond to DWIA (solid) and PWIA (dashed) calculations. The incident pion energy is given at the top and one outgoing proton is fixed at  $50^\circ$ . The second proton is at the quasifree angle for which zero recoil momentum for the residual nucleus is kinematically allowed.

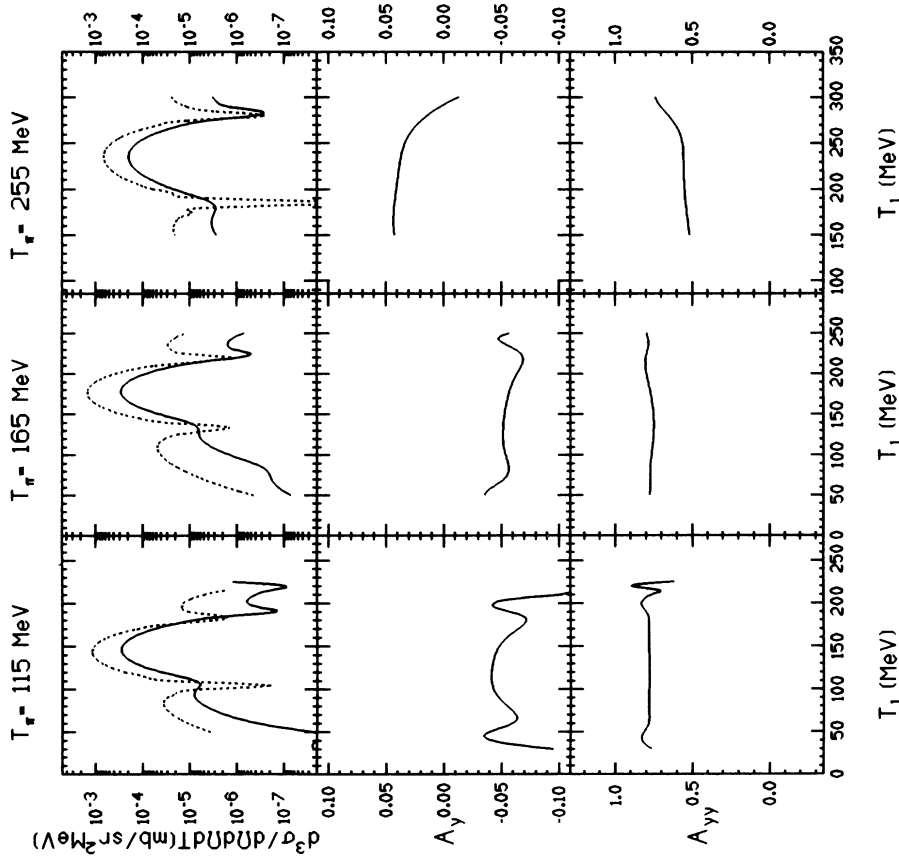


FIG. 4. Energy sharing cross sections, vector analyzing powers ( $A_y$ ), and tensor analyzing powers ( $A_{yy}$ ) for  $^{14}\text{N}(\pi^+, 2p)^{12}\text{C}(0^-)$  with  $L=1$  transfer. The curves correspond to DWIA (solid) and PWIA (dashed) calculations. The incident pion energy is given at the top and one outgoing proton is fixed at  $50^\circ$ . The second proton is at the quasifree angle.

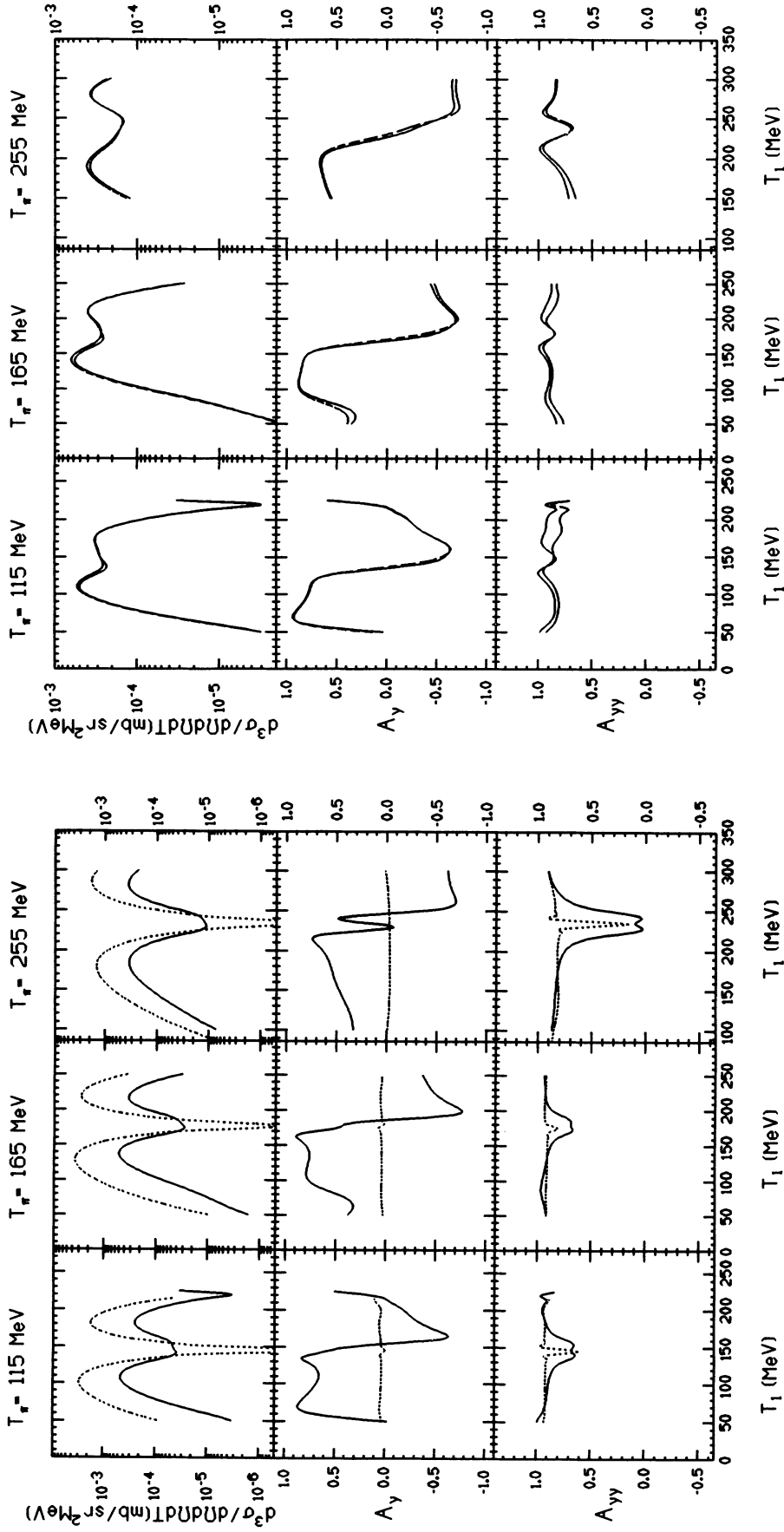


FIG. 5. Energy sharing cross sections, vector analyzing powers ( $A_y$ ), and tensor analyzing powers ( $A_{yy}$ ) for  $^{14}\text{N}(\pi^+, 2p)^{12}\text{C}(0^+)$  with  $L=2$  transfer. The curves correspond to DWIA (solid) and PWIA (dashed) calculations. The incident pion energy is given at the top and one outgoing proton is fixed at  $50^\circ$ . The second proton is at the quasifree angle.

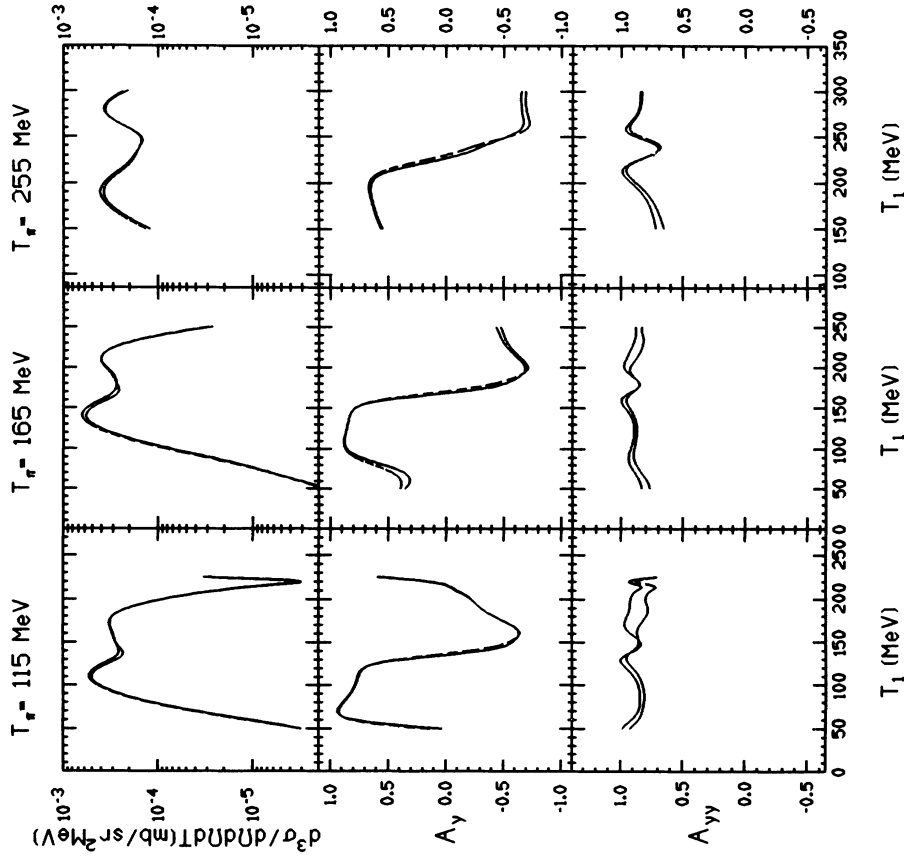


FIG. 6. Energy sharing cross sections, vector analyzing powers ( $A_y$ ), and tensor analyzing powers ( $A_{yy}$ ) for  $^{14}\text{N}(\pi^+, 2p)^{12}\text{C}(0^+)$ . The kinematic conditions are as in Fig. 5. The curves correspond to DWIA calculations with (dashed) and without (solid) spin-orbit potentials for the outgoing protons.

[24]. The results for the ground-state transition  $^{14}\bar{N}(\pi^+, 2p)^{12}\text{C}(0^+, 0.0 \text{ MeV})$  are shown as the solid curves in Fig. 6. The dotted curves are obtained by setting the spin-orbit potential for the outgoing protons to zero. It is seen that the spin-orbit effects are negligible, and hence, the expressions derived in Sec. II for the  $L=0$  and 1 transitions are valid in discussing the results presented in preceding figures. Similar small effects due to the spin-orbit potentials for emitted protons are also observed in DWIA calculations of  $A(\pi, \pi p)$  [8] and  $A(p, 2p)$  [25] reactions. We have omitted the spin-orbit potentials in the remainder of the calculations.

The most interesting result in Fig. 6 is that the predicted analyzing power  $A_y$  is very large and is certainly within experimental reach. This is due to the fact that the transition to the ground state of  $^{12}\text{C}$  is predominantly an  $L=2$  transition which is influenced strongly by distortion, as seen in Fig. 5. This important feature is further illustrated in Fig. 7, in which the dotted curves are obtained by arbitrarily enhancing the  $L=0$  component of the Cohen and Kurath nuclear structure amplitude by a

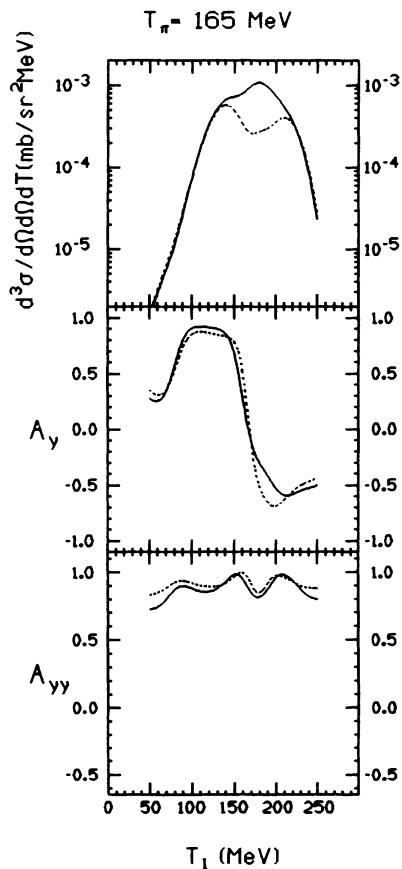


FIG. 7. Energy sharing sections, vector analyzing powers ( $A_y$ ), and tensor analyzing powers ( $A_{yy}$ ) for  $^{14}\bar{N}(\pi^+, 2p)^{12}\text{C}(0^+, \text{g.s.})$  at 165 MeV incident pion energy. The curves correspond to DWIA calculations for the Cohen-Kurath wave functions (dashed lines) and with the  $L=0$  amplitude doubled (solid lines). The geometry is the same as Fig. 3.

factor of 2. We see that the predicted  $A_y$  is largely unaffected by the increase in the contribution from  $L=0$  (see Fig. 3). Therefore, a precise measurement of  $A_y$  will provide a good test of our treatment of distortion effects.

Our predictions for  $^{14}\bar{N}(\pi^+, 2p)^{12}\text{C}(2^+, 4.43 \text{ MeV})$  are displayed in Fig. 8. Here the  $L=0$  and 2 contributions are comparable, and hence the distortion effects on analyzing powers are less dramatic. Measurements for this transition are, of course, also desirable for a more complete study of the role of distortion effects in the reaction dynamics.

### C. Predictions for possible $\bar{A}(\pi^+, 2p)$ experiments

To stimulate the planning of new experiments which address the pion absorption mechanism, we also carry out calculations for  $^6\text{Li}$ ,  $^7\text{Li}$ , and  $^{13}\text{C}$  targets. All have been successfully polarized for use in nuclear reaction studies.

(1)  $^6\bar{\text{Li}}(\pi^+, 2p)^4\text{He}$ . For this transition to the  $^4\text{He}$  ground state we used a simple  $\alpha$ - $d$  cluster model to describe the  $^6\text{Li}$  target. Such a description has had some success in the past in describing  $(p, pd)$  [26] and  $(p, p\alpha)$  [27] reactions on  $^6\text{Li}$ . The DWIA results are shown in Fig. 9. Not surprisingly, given the choice of a cluster model and the weak deuteron binding energy, the analyzing powers are just those of  $\pi^+ d \rightarrow pp$  smeared slightly by the Fermi motion which is small. Again because of the structure and the narrow momentum distribution of the deuteron, the peak cross section is quite large. Thus  $^6\text{Li}$  is a good nucleus with which to begin a study of pion absorption on polarized nuclei and to look for deviations from simple absorption on a deuteron. These could arise from a variety of sources, such as the internal structure of the  $n$ - $p$  pair or an  $L=2$   $\alpha$ - $d$  component where even a small amplitude can have a large effect on the vector analyzing power.

(2)  $^7\text{Li}(\pi^+, 2p)^5\text{He}$ . Calculations for the ground state transition ( $\frac{3}{2}^- \rightarrow \frac{3}{2}^-$ ) are presented in Fig. 10. Spectroscopic amplitudes were calculated assuming that the  $^7\text{Li}$  ground state is well described in  $LS$  coupling by a  $\{3\}^2 P_{3/2}$  wave function. This term has an amplitude of  $\sim 0.98$  in typical nuclear structure calculations [24,28]. At low recoil momentum (near the peak in the cross section) the cross section is dominated by  $L=0$ . However, the  $L=2$  component is large and dominates as the recoil momentum increases (energies above and below the peak). Because the  $L=2$  vector analyzing power is so much larger than that for  $L=0$ ,  $A_y$  corresponds principally to  $L=2$ , except very near the minimum recoil momentum point. In the tensor analyzing power one sees clear contributions from the two  $L$  transfers in the regions where they dominate.

Transitions to the excited states of  $^5\text{He}$  are also expected to be strong. We have carried out one such calculation for the  $\frac{3}{2}^+$  state at 16.8 MeV, by assuming the removal of a  $(1s1p)$  pair with angular momentum  $L=1$  relative to the core. The residual state was assumed to be described by coupling the  $s$ -shell hole to two  $p$ -shell nucleons in a  $\{2\}^3 S_1$  state. With these structure assumptions  $J=0, 1$ , and 2 terms all contribute with comparable

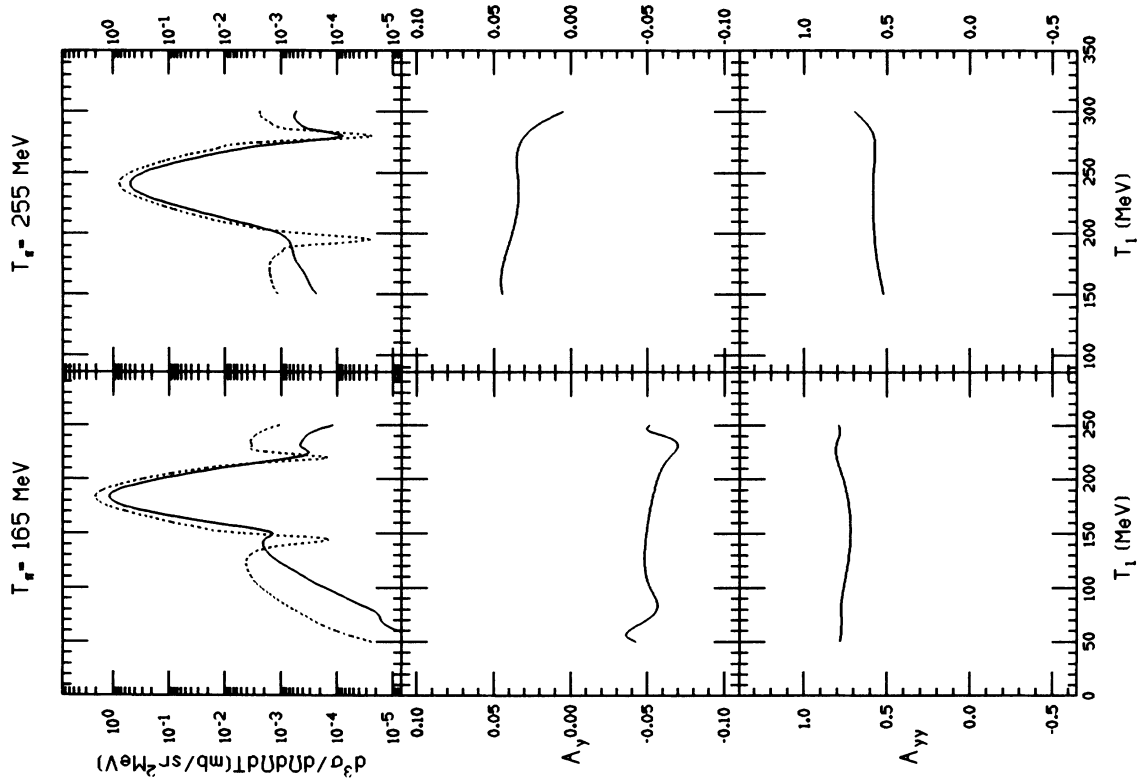


FIG. 9. Energy sharing cross sections, vector analyzing powers ( $A_y$ ), and tensor analyzing powers ( $A_{yy}$ ) for  ${}^6\text{Li}(\pi^+, 2p){}^4\text{He}(0^+, g.s.)$  with  $L=0$  transfer. The curves correspond to DWIA (solid) and PWIA (dashed) calculations. The incident pion energy is given at the top and one outgoing proton is fixed at  $50^\circ$ . The second proton is at the quasifree angle.

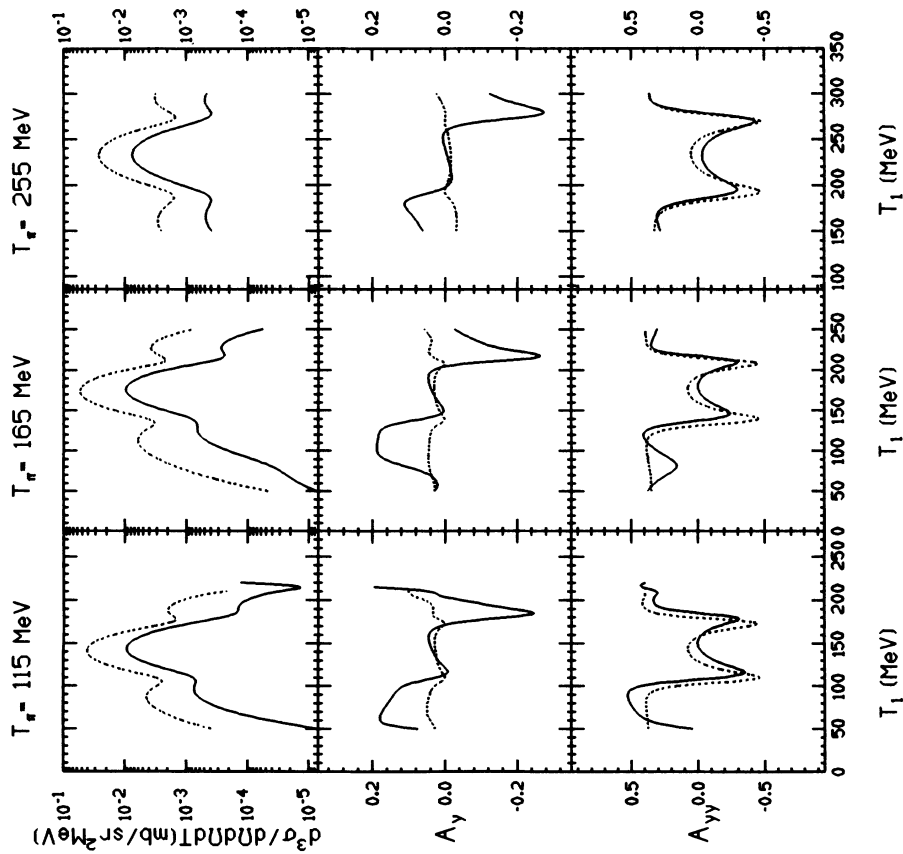


FIG. 8. Energy sharing cross sections, vector analyzing powers ( $A_y$ ), and tensor analyzing powers ( $A_{yy}$ ) for  ${}^{14}\text{Ni}(\pi^+, 2p){}^{12}\text{C}(2^+, 4.43 \text{ MeV})$ . The curves correspond to DWIA (solid) and PWIA (dashed) calculations. The incident pion energy is given at the top and one outgoing proton is fixed at  $50^\circ$ . The second proton is at the quasifree angle.

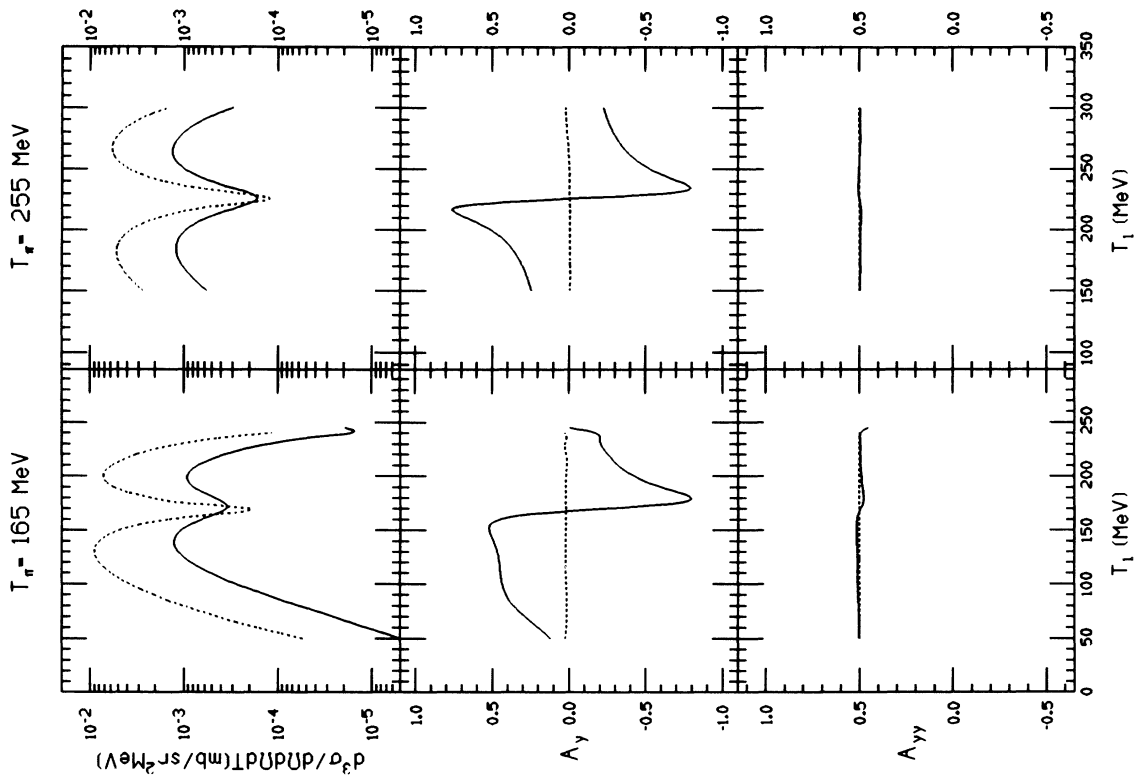


FIG. 11. Energy sharing cross sections, vector analyzing powers ( $A_y$ ), and tensor analyzing powers ( $A_{yy}$ ) for  ${}^7\text{Li}(\pi^+, 2p){}^5\text{He}(\frac{3}{2}^+, 16.6 \text{ MeV})$ . The curves correspond to DWIA (solid) and PWIA (dashed) calculations. The incident pion energy is given at the top and one outgoing proton is fixed at  $50^\circ$ . The second proton is at the quasi-free angle.

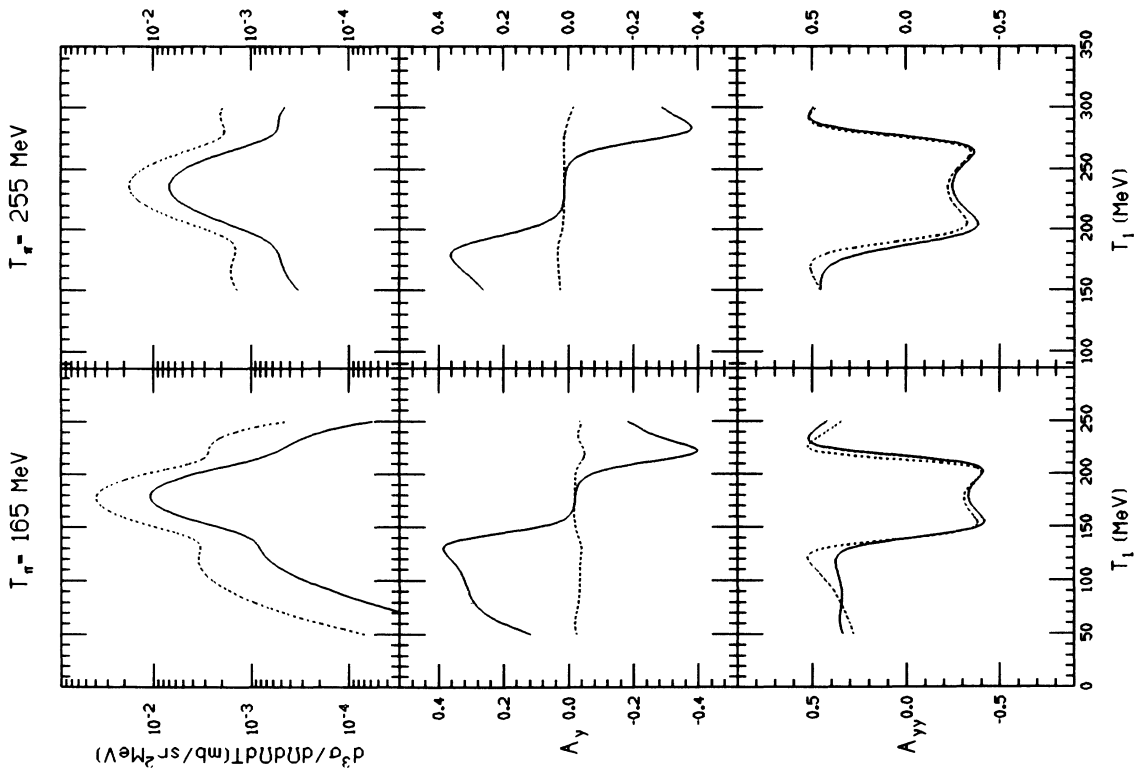


FIG. 10. Energy sharing cross sections, vector analyzing powers ( $A_y$ ), and tensor analyzing powers ( $A_{yy}$ ) for  ${}^7\text{Li}(\pi^+, 2p){}^5\text{He}(\frac{3}{2}^-, \text{g.s.})$ . The curves correspond to DWIA (solid) and PWIA (dashed) calculations. The incident pion energy is given at the top and one outgoing proton is fixed at  $50^\circ$ . The second proton is at the quasifree angle.

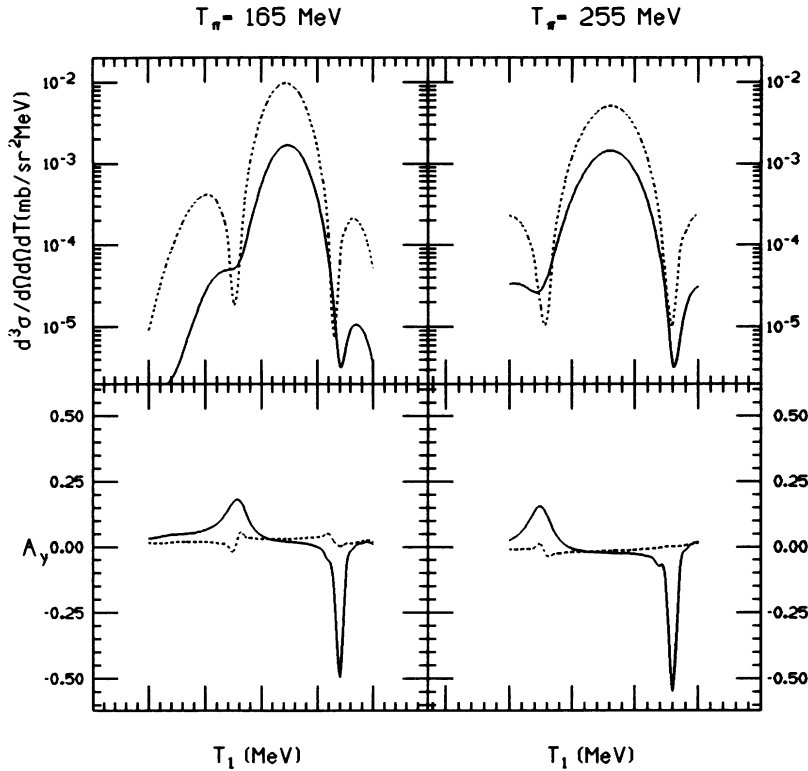


FIG. 12. Energy sharing cross sections, vector analyzing powers ( $A_y$ ), and tensor analyzing powers ( $A_{yy}$ ) for  $^{13}\text{C}(\pi^+, 2p)^{11}\text{B}(\frac{3}{2}^-, \text{g.s.})$ . The curves correspond to DWIA (solid) and PWIA (dashed) calculations. The incident pion energy is given at the top and one outgoing proton is fixed at  $50^\circ$ . The second proton is at the quasifree angle.

amplitudes. These results are presented in Fig. 11, and are similar to those for  $^{14}\text{N}$  with  $L=1$  (Fig. 4), although the magnitude of the analyzing powers differ due to the initial and final nuclear spins.

(3)  $^{13}\text{C}(\pi^+, 2p)^{11}\text{B}$ . For the ground state we have a  $\frac{1}{2}^-$  to  $\frac{3}{2}^-$  transition. This can proceed by a combination of  $L=0$  or 2 and with  $J=1, 2$ , or 3, the relative contributions being determined by the  $p$ -shell wave functions. Calculations using the Cohen-Kurath wave functions are shown in Fig. 12. In this case, unlike that of the  $^7\text{Li}$  ground-state transition, we see that the  $L=0$  component dominates leading to very small analyzing powers. Only in the cross section minima does one see contributions from  $L=2$  to the analyzing power.

#### IV. SUMMARY AND CONCLUSIONS

We have presented the DWIA formalism and calculations of cross sections, and vector and tensor analyzing powers for pion absorption on polarized nuclear targets. In this we have assumed that the absorption takes place on  $^3S_1$ ,  $T=0$   $np$  pairs. The amplitudes for the  $\pi^+(np) \rightarrow pp$  process were taken from the work of Bugg and co-workers [17], who have fitted experimental data for the  $\pi^+d \rightarrow pp$  reaction. In calculations of  $^{16}\text{O}(\pi^+, 2p)^{14}\text{N}$  we have shown that the use of these amplitudes leads to a reduction in the  $J$  dependence observed in previous works.

The primary motivation for this work was to provide guidance in the design of new experiments which attempt to understand two-nucleon pion absorption. The ability

to measure analyzing powers using polarized targets should provide new sensitivities to the reaction dynamics through the interference terms inherent in analyzing powers.

For relatively simple cases we have shown that contributions to the vector analyzing power arise both from the two-body  $\pi^+(np) \rightarrow pp$  process and from the distortion of the incoming pion and outgoing protons by the residual nucleus. For the case of  $L=0$  transitions, no distortion effects contribute to the vector analyzing power. This makes such transitions excellent candidates for studies of the fundamental two-nucleon absorption process in nuclei. Unfortunately, the vector analyzing power is small, so that a high quality experiment will be required.

For nonzero  $L$  transfers distortions dominate and lead to quite large analyzing powers. Thus such transitions provide the opportunity to study the overall treatment of the reaction mechanism, particularly the treatment of the distortion of the incoming and outgoing particles. An  $L=1$  transition is particularly attractive for such studies, since the vector analyzing powers are zero if there is no distortion.

The tensor analyzing power appears to be rather insensitive to distortion effects and is, therefore, another candidate for studies of the  $\pi^+(pn) \rightarrow pp$  process in the nuclear medium. However, at the present time such experiments are impractical.

Finally, if one can understand the reaction dynamics better, there are nuclear structure aspects to such measurements. Due to the large differences between the  $L=0$  and 2 vector analyzing powers, a measurement of

$A_y$  could serve to constrain nuclear structure calculations which determine the relative amplitudes for  $L=0$  and 2.

We have also presented a series of calculations for specific transitions for a variety of nuclei which have been polarized. These calculations will hopefully be helpful in the planning of experiments.

#### ACKNOWLEDGMENTS

Support for this work has been provided in part by the National Science Foundation and the U.S. Department of Energy, Nuclear Physics Division, under Contract W-31-109-ENG-38.

#### APPENDIX

The two-body  ${}^2\text{H}(\pi^+, 2p)$  cross sections have been calculated using the parametrizations of Bugg and co-workers [17]. This parametrization provides  ${}^2\text{H}(\pi^+, 2p)$  cross sections comparable to those of Ritchie [23]. We also find that the vector analyzing power for  ${}^2\text{H}(\pi^+, 2p)$  calculated from Bugg and co-workers is in good agreement with the published data of Smith *et al.* [29].

Following the formalism of Mandl and Regge [30], we write the  $S$  matrix as

$$S = \sum_{ij} \psi_f \mu_{Jl_\pi l_p} \psi_i^\dagger,$$

where the elements of this matrix can be written more explicitly as

$$\begin{aligned} S(m_d, M_p) = & \sum_{l_\pi l_p} (l_p(m_d - M_p) S M_p | J m_d) \\ & \times a_{Jl_\pi l_p}(l_\pi 0 | m_d | J m_d) \\ & \times Y_{l_p}^{m_d - M_p}(\theta, \phi) Y_{l_\pi}^0(0, 0). \end{aligned}$$

We have chosen the axis of symmetry ( $\hat{z}$ ) along the incoming beam;  $l_\pi$  and  $l_p$  are the relative orbital angular

momenta in the entrance channel ( $\pi d$ ) and the exit channel ( $pp$ ), respectively. The quantum numbers  $m_d$  and  $M_p$  are, respectively, the spin states of the deuteron and the  $pp$  multiplet (triplet or singlet). The quantity  $J$  is the total angular momentum of the  $\pi d$  or  $pp$  system. Angular momentum conservation and parity restrict  $l_\pi = l_p \pm 1$  [30].

The quantity  $a_{Jl_\pi l_p}$  are the pion production amplitudes and are related to the matrix elements  $\mu_{Jl_\pi l_p}$  by

$$a_{Jl_\pi l_p} = \sqrt{(2l_p + 1)/4\pi} \mu_{Jl_\pi l_p}.$$

These production amplitudes are taken from the phenomenological work of Bugg and co-workers [17] who have tabulated the amplitudes for a range of energies, 400–800 MeV in the  $pp$  laboratory system. We use a spline interpolation for intermediate energies. Since these amplitudes are for  $pp \rightarrow \pi^+ d$ , we need to evaluate the amplitudes at a proton laboratory energy  $T_p$ , given a pion laboratory incident energy  $T_\pi$  (the deuteron is assumed at rest); we obtain

$$T_p = \left[ \frac{m_\pi^2 + m_d^2 - 2m_p^2 + 2m_d(T_\pi + m_\pi)}{2m_p} \right] - m_p.$$

We can then write the differential cross section for  $\pi d \rightarrow pp$  as

$$\frac{d\sigma}{d\Omega}(\pi d \rightarrow pp) = \frac{1}{3} \left[ \frac{4\pi}{k_\pi} \right]^2 \sum_{m_d M_p} 10 |S(m_d, M_p)|^2,$$

where  $k_\pi$  is the c.m. pion incident momentum in  $(\text{fm})^{-1}$ . Here we have used detailed balance to relate pion absorption and production cross sections:

$$\frac{d\sigma}{d\Omega}(\pi d \rightarrow pp) = \frac{4}{3} \left[ \frac{k_p}{k_\pi} \right]^2 \frac{d\sigma}{d\Omega}(pp \rightarrow \pi d),$$

where  $k_p$  is the proton momentum in the c.m. system.

- 
- [1] B. Larson, O. Häusser, E. J. Brash, C. Chan, A. Rahav, C. Bennhold, P. P. J. Belheij, R. S. Henderson, B. K. Jennings, A. Mellinger, D. Ottewell, A. Trudel, M. C. Vetterli, D. M. Whittal, S. Ram, L. Tiator, and S. S. Kamalov, *Phys. Rev. Lett.* **67**, 3356 (1991).
- [2] S. Ritt, E. T. Boschitz, R. Meier, R. Tacik, M. Wessler, K. Junker, J. A. Konter, S. Mango, D. Renker, B. van den Brandt, V. Efimov, A. Kovaljov, A. Prokofiev, R. Mark, P. Chaumette, P. Deregel, G. Durand, J. Fabve, and W. Thiel, *Phys. Rev. C* **43**, 745 (1991).
- [3] Yi-Fen Yen, B. Brinkmüller, D. Dehnard, S. M. Sterbenz, Yi-Ju Yu, Brian Berman, G. R. Burlinson, K. Cranston, A. Klein, G. S. Kyle, R. Alarcon, T. Averett, J. R. Comfort, J. J. Görden, B. G. Ritchie, J. R. Tinsley, M. Barlett, G. W. Hoffmann, K. Johnson, C. F. Moore, M. Purcell, H. Ward, A. Williams, J. A. Faucett, S. J. Greene, J. J. Jarmer, J. A. McGill, C. L. Morris, S. Penttilä, N. Tanaka, H. T. Fortune, E. Insko, R. Ivie, J. M. O'Donnell, D. Smith, M. A. Khandaker, and S. Chakravarti, *Phys. Rev. Lett.* **66**, 1959 (1991).
- [4] R. Tacik, E. T. Boschitz, R. Meier, S. Ritt, M. Wessler, K. Junker, J. A. Konter, S. Mango, D. Renker, B. van den Brandt, W. Meyer, W. Thiel, P. Chaumette, J. Deregel, G. Durand, J. Fabre, P. Amaudruz, R. R. Johnson, G. Smith, P. Weber, and R. Mach, *Phys. Rev. Lett.* **63**, 1784 (1989); R. Meier, E. T. Boschitz, S. Ritt, R. Tacik, M. Wessler, J. A. Konter, S. Mango, D. Renker, B. van den Brandt, W. Meyer, W. Thiel, R. Mach, P. Amaudruz, R. R. Johnson, G. R. Smith, and P. Weber, *Phys. Rev. C* **42**, 2222 (1990).
- [5] J. J. Görden, J. R. Comfort, J. R. Tinsley, T. Averett, J. DeKorse, B. Franklin, B. G. Ritchie, G. Kyle, A. Klein, B. Berman, G. Burlinson, K. Cranston, J. A. Faucett, J. J. Jarmer, J. N. Knudson, S. Penttilä, N. Tanaka, B. Brinkmüller, D. Dehnard, Yi-Fen Yen, S. Höibråten, H. Breuer, B. S. Flanders, M. A. Khandaker, D. L. Naples, D. Zhang, M. L. Barlett, G. W. Hoffmann, and M. Purcell, *Phys. Rev. Lett.* **66**, 2193 (1991).
- [6] P. B. Siegel and W. R. Gibbs, *Phys. Rev. C* **36**, 2473 (1987).
- [7] H. C. Newns, *Proc. Phys. Soc. London Sect. A* **66**, 477

- (1953); H. C. Newns and M. Y. Refai, *ibid.* **71**, 627 (1958).
- [8] N. S. Chant and P. G. Roos, *Phys. Rev. C* **38**, 787 (1988).
- [9] N. S. Chant and P. G. Roos, *Phys. Rev. C* **39**, 957 (1989).
- [10] D. J. Mack, P. G. Roos, H. Breuer, N. S. Chant, S. D. Hyman, F. Khazaie, B. G. Ritchie, J. D. Silk, G. S. Kyle, P. A. Amaudruz, Th. S. Bauer, C. H. Q. Ingram, D. Renker, R. A. Schumacher, U. Sennhauser, and W. J. Burger, *Phys. Rev. C* **45**, 1767 (1992).
- [11] R. A. Schumacher, P. A. Amaudruz, C. H. Q. Ingram, U. Sennhauser, H. Breuer, N. S. Chant, A. E. Feldman, B. S. Flanders, F. Khazaie, D. J. Mack, P. G. Roos, J. D. Silk, and G. S. Kyle, *Phys. Rev. C* **38**, 2205 (1988).
- [12] G. Backenstoss, M. Izycki, P. Salvisberg, M. Steinacher, P. Weber, H. J. Weyer, S. Cierjacks, S. Ljungfelt, H. Ullrich, M. Furie, and T. Petkovic, *Phys. Rev. Lett.* **55**, 2782 (1985).
- [13] K. A. Aniol, A. Altman, R. R. Johnson, H. W. Roser, R. Tacik, U. Wienands, D. Ashery, J. Alster, M. A. Moines-ter, E. Piasetzky, D. R. Gill, and J. Vincent, *Phys. Rev. C* **33**, 1714 (1986).
- [14] S. Mukhopadhyay, S. Levenson, R. E. Segel, G. Garino, D. Geesaman, J. P. Schiffer, G. Stephans, B. Zeidman, E. Ungricht, H. Jackson, R. Kowalczyk, D. Ashery, E. Paisetsky, M. Moines-ter, I. Navon, L. C. Smith, R. C. Minehart, G. S. Das, R. R. Whitney, R. McKeown, B. Anderson, R. Madey, and J. Watson, *Phys. Rev. C* **43**, 957 (1991).
- [15] K. Ohta, M. Thies, and T.-S. H. Lee, *Ann. Phys. (N.Y.)* **163**, 420 (1985).
- [16] H. Garcilazo and T. Mizutani,  *$\pi NN$  Systems* (World Scientific, Singapore, 1990).
- [17] D. V. Bugg, A. Hasan, and R. L. Shypit, *Nucl. Phys.* **A477**, 546 (1988).
- [18] P. Kitching, W. J. McDonald, Th. A. J. Maris, and C. A. Z. Vasconcellos, in *Advances in Nuclear Physics*, edited by J. W. Negele and E. Vogt (Plenum, New York, 1985), Vol. 15, p. 43.
- [19] L. R. B. Elton and A. Swift, *Nucl. Phys.* **A94**, 52 (1967).
- [20] A. Nadasen, P. G. Roos, N. S. Chant, A. A. Cowley, C. Samanta, and J. Wesick, *Phys. Rev. C* **23**, 2353 (1981).
- [21] C. Samanta, N. S. Chant, P. G. Roos, A. Nadasen, J. Wesick, and A. A. Cowley, *Phys. Rev. C* **34**, 1610 (1986).
- [22] W. B. Cottingham and D. B. Holtkamp, *Phys. Rev. Lett.* **45**, 1828 (1980).
- [23] B. G. Ritchie, *Phys. Rev. C* **44**, 533 (1991).
- [24] S. Cohen and D. Kurath, *Nucl. Phys.* **A141**, 145 (1970).
- [25] N. S. Chant and P. G. Roos, *Phys. Rev. C* **27**, 1060 (1983).
- [26] R. E. Warner, J. Q. Yang, D. L. Friesel, P. Schwandt, G. Caskey, A. Galonsky, B. Remington, A. Nadasen, N. S. Chant, F. Khazaie, and C. Wang, *Nucl. Phys.* **A443**, 64 (1985).
- [27] P. G. Roos, D. A. Goldberg, N. S. Chant, R. Woody III, and W. Reichart, *Nucl. Phys.* **A257**, 317 (1976).
- [28] A. N. Boyarkina, *Bull. Acad. Sci. USSR Phys. Ser.* **28**, 255 (1964).
- [29] G. R. Smith, E. L. Mathie, E. T. Boschitz, C. R. Ottermann, W. Gyles, W. List, S. Mango, J. A. Konter, B. van den Brandt, R. Olszewski, and R. R. Johnson, *Phys. Rev. C* **30**, 980 (1984).
- [30] F. Mandl and T. Regge, *Phys. Rev.* **99**, 1478 (1955).